Homogenization-based modelling of reinforced concrete in the context of durability-oriented analyses

E. Rumanus & G. Meschke
Institute for Structural Mechanics, Ruhr University Bochum, Bochum, Germany

ABSTRACT: In the context of a poromechanics framework developed for durability-oriented analysis, the paper is mainly concerned with a constitutive model for reinforced concrete. A continuous concrete matrix and two different sets of steel reinforcement characterize the three-phase composite material. For each phase, the nonlinear pre- and post-peak behavior is described separately, while considering interactions between the reinforcement bars and the concrete. The material behaviour of the matrix material is formulated by a combined multisurface elasto-plastic damage model. A classical J_2–plasticity flow rule describes the elasto-plastic response of the steel reinforcement. Based on continuum micromechanics, the Mori-Tanaka homogenization technique is considered as a suitable approach to derive the homogenized (macromechanical) constitutive relations of the composite material and related local (micromechanical) field information which is essential for durability analyses. Dowel action between the reinforcement bars and the concrete is implicitly captured by the chosen approach. The model performance is demonstrated by selected numerical and experimental studies.

1 INTRODUCTION

Corrosion of the reinforcement constitutes one of the major limiting factors for the durability of reinforced concrete structures. Expansive radial pressures induced by corrosion products (rust) along the interface between the steel bars and the concrete may cause cracking and spalling of cover concrete. Gradual loss of bond strength between the reinforcement and the surrounding concrete and the reduction of reinforcement cross-sectional area amplify the deterioration mechanisms caused by corrosion. On the structural level, a reduction of the structural stiffness and of the load carrying capacity affects the (residual) service life-time of reinforced structures and may lead to premature failure. Since the nature of steel corrosion is physico-chemical and its evolution is strongly moisture dependent, life-time oriented structural analyses require consideration of transport mechanisms of moisture and of corrosive substances such as chloride ions or calcium hydroxide leading to the depassivation of the reinforcement bars. Equally relevant is a suitable model for reinforced concrete allowing to represent the interacting mechanisms between the reinforcement bars and the surrounding concrete such as bond slip and dowel action as well as the corrosion-induced degradation of these interaction properties.

In this study, the main focus is laid on the latter aspect: Reinforced concrete is modelled as a three-phase composite material consisting of a continuous matrix and two different sets of rebars. This idea has been suggested recently by (Pietruszczak and Winnicki 2003) and (Linero et al. 2006) using the classical *mixture theory* in order to obtain macroscopic properties of the composite material. In the present paper, the macroscopic behavior of this composite material is obtained by employing homogenization schemes to a representative volume element (RVE), in which the necessary conditions for the application of homogenization are fulfilled (Zaoui 2002). This model for reinforced concrete is being implemented within a multiphase model for partially saturated concrete accounting for heat and moisture transport and the relevant interactions observed on the nano- and micro-level between cracking, drying and creep (Meschke and Grasberger 2003; Grasberger and Meschke 2004).

While for mainly unidirectional loading a 1D-modelling of the reinforcement within an embedded approach would be sufficient (Linero et al. 2006), shear stresses transmitted by the rebar in case of cracked concrete (dowel action) suggest a homogenization approach using a fully 3D representation of the steel reinforcement within the considered RVE. Effects such as dowel-action are therefore captured automatically without any additional specifications of

the residual shear stiffness in cracked zones.

The mechanical response of composite materials is highly influenced by the morphology of the microstructure, the properties of the constituents and by micromechanical interactions within the composite. The volume fraction, the aspect ratio, the orientation and the shape of constituents with correlated interactions have to be taken into account in order to describe the structural response accurately. To avoid modelling of the complex heterogeneous microstructure, adequate homogenization techniques are performed. Based on continuum micromechanics (Zaoui 2002) the MORI-TANAKA homogenization scheme is employed in this study in order to provide an estimate of the constitutive relations of reinforced concrete described as a three-phase composite material. The adopted micromechanical model ensures the continuity of the surrounding matrix and accounts for interactions between the embedded inhomogeneities (Mori and Tanaka 1973).

The main goal of this study is to derive a reliable macroscopic model for reinforced concrete as a composite material which provides information about the stress and strain fields of the individual constituents (the concrete matrix and the reinforcement bars). This information is essential when degradation mechanisms originating from mechanical, physical and physico-chemical processes have to be estimated accurately. Since details on the coupled hygro-mechanical model for concrete have been already presented elsewhere (Meschke and Grasberger 2003; Grasberger and Meschke 2004), the focus of this paper lies on the formulation of reinforced concrete based on homogenization micromechanical approach. Since this work is in progress, in a first version of the proposed model, bond-slip between the rebar and the surrounding concrete is not yet accounted for.

2 CONSTITUTIVE MODELS

2.1 *Concrete matrix material*

For describing damage and creep of cementitious materials subjected to external loading and changing hygral conditions an elasto-plastic damage model (Meschke and Grasberger 2003; Grasberger and Meschke 2004) formulated within the framework of the BIOT-COUSSY theory (Coussy 2004) is employed. Concrete is assumed to consist of a continuous matrix and pores, which, depending on the environmental conditions, are in general partially filled by liquid water and by an ideal mixture of water vapour and dry air. Based on the considered theory, the individual phases formed by the matrix phase and the pores are represented as a homogeneous material according to their volume fraction in each material point. The related constitutive relations capturing the main physical processes acting on the nano- and mi-

crolevel are obtained by means of defining an appropriate expression for the free energy of the thermodynamic system together with macroscopic coupling coefficients which are obtained from relating micro- and macroscopic quantities and exploiting symmetry conditions of the macroscopic energy function Ψ_m

$$
\begin{aligned}
\Psi_m \quad = \quad & \mathcal{W}(\boldsymbol{\varepsilon}_m - \boldsymbol{\varepsilon}_m^p - \boldsymbol{\varepsilon}_m^f, m_l - \rho_l\phi_l^p, \psi, \gamma_f, T) \\
& + \mathcal{U}(\alpha_R, \alpha_{DP})
\end{aligned} \tag{1}
$$

for the matrix material (Grasberger and Meschke 2004). The index m refers to the matrix. The linearized strain tensor $\boldsymbol{\varepsilon}_m$ within the matrix is assumed to be small and can therefore be decomposed into elastic strains $\boldsymbol{\varepsilon}_m^e$, plastic strains $\boldsymbol{\varepsilon}_m^p$ and long-term creep strains $\boldsymbol{\varepsilon}_m^f$ i.e.

$$
\boldsymbol{\varepsilon}_m = \boldsymbol{\varepsilon}_m^e + \boldsymbol{\varepsilon}_m^p + \boldsymbol{\varepsilon}_m^f. \tag{2}
$$

Moisture distribution is described by the liquid mass content m_l and by liquid, with a density of ρ_l, occupying the non-recoverable portion of the porosity ϕ_l^p. The integrity ψ captures the isotropic damage state of the poromechanical material. Viscous slip γ_f, associated with relative motions within gel-pores, causes creep deformations observed on the macroscopic scale (Bažant et al. 1997; Grasberger and Meschke 2003). The thermal field is described by the absolute temperature T. The hardening and softening law, specifying the material behaviour beyond the elastic domain, is governed by the internal variables α_R for tension cracking and by α_{DP} for compression damage.

A multi-surface fracture energy-based damage-plasticity theory is employed to characterize the behaviour of concrete in tension and compression (Meschke et al. 1998). Degradation mechanisms and inelastic deformations are controlled by four threshold functions f_k defining a region of admissible stress states in the space of plastic effective stresses $\boldsymbol{\sigma}_m'$

$$
\mathbf{E} = \{(\boldsymbol{\sigma}_m', q_k) | f_k(\boldsymbol{\sigma}_m', q_k(\alpha_k)) \leq 0, \ k = 1, .., 4\}. \tag{3}
$$

Cracking of concrete is accounted for by means of a fracture energy based Rankine criterion, employing three failure surfaces perpendicular to the axes of principal stresses

$$
f_{R,A}(\boldsymbol{\sigma}_m', q_R) = \sigma_A' - q_R(\alpha_R) \leq 0, \quad A = 1, 2, 3 \tag{4}
$$

with $q_R(\alpha_R) = -\partial\mathcal{U}/\partial\alpha_R$ denoting the softening parameter and the index A refers to the principal direction. The ductile behaviour of concrete subjected to compressive loading is described by a hardening/softening Drucker-Prager plasticity model

$$
f_{DP}(\boldsymbol{\sigma}_m', q_{DP}) = \sqrt{J_2} - \kappa_{DP}I_1 - \frac{q_{DP}(\alpha_{DP})}{\gamma_{DP}} \leq 0 \tag{5}
$$

with $q_{DP}(\alpha_{DP}) = -\partial \mathcal{U} / \partial \alpha_{DP}$ as the hardening/softening parameter and the values κ_{DP} and γ_{DP} are obtained from the compressive strength of the material.

The mechanical behavior for the matrix in case that no moisture and heat transport is considered, is characterized by the stress field of the matrix $\boldsymbol{\sigma}_m$ which is equal to the plastic effective stress tensor $\boldsymbol{\sigma}'_m$ (Grasberger and Meschke 2004) and is obtained from equation (1) and (2) as

$$\boldsymbol{\sigma}_m = \psi \, \boldsymbol{\mathcal{C}}_m : \boldsymbol{\varepsilon}_m^e = \psi \, \boldsymbol{\mathcal{C}}_m : (\boldsymbol{\varepsilon}_m - \boldsymbol{\varepsilon}_m^p - \boldsymbol{\varepsilon}_m^f) \qquad (6)$$

with $\boldsymbol{\mathcal{C}}_m$ as the undamaged elasticity tensor of the matrix material.

2.2 *Reinforcement*
Similar to equation (2), the total strain tensor of the rebar $\boldsymbol{\varepsilon}_s$ can be decomposed into an elastic $\boldsymbol{\varepsilon}_s^e$ and a plastic part $\boldsymbol{\varepsilon}_s^p$

$$\boldsymbol{\varepsilon}_s = \boldsymbol{\varepsilon}_s^e + \boldsymbol{\varepsilon}_s^p. \qquad (7)$$

The subscript s refers to the deformations of the steel. Since the distribution of the stiffness within a reinforced concrete structure is discontinuous, the strains of the matrix given in equation (2) may differ from the strains of the reinforcement even when full bonding between reinforcement and matrix is assumed. The stress-strain relationship is obtained from the stored energy function Ψ_s as

$$\boldsymbol{\sigma}_s = \partial \, \Psi_s / \partial \, \boldsymbol{\varepsilon}_s^e = \boldsymbol{\mathcal{C}}_s : \boldsymbol{\varepsilon}_s^e = \boldsymbol{\mathcal{C}}_s : (\boldsymbol{\varepsilon}_s - \boldsymbol{\varepsilon}_s^p), \qquad (8)$$

where $\boldsymbol{\mathcal{C}}_s$ denotes the isotropic tensor of elasticity. The admissible stress field $\boldsymbol{\sigma}_s$ within the rebar is described by a classical J_2-plasticity model (Simo and Hughes 1998) and the non-linear regime beyond the yield stress σ_y is governed by an isotropic linear hardening law based on the von Mises yield condition

$$f(\mathbf{s}, \alpha) = \| \mathbf{s} \| - \sqrt{2/3} \, [\sigma_y + K \, \alpha] \le 0. \qquad (9)$$

The evolution of the isotropic hardening is governed by the internal variable α and by the constant isotropic hardening plastic modulus K.

3 CONTINUUM MICROMECHANICS
3.1 *Composite material (reinforced concrete)*
In this study, the considered three-phase composite consists of a continuous matrix formed by concrete and by two sets of straight rebars representing the steel reinforcement forming the reinforcement-layer. The direction of the rebars and the geometry of the cross section may be arbitrary within the 2-3–plane of the reinforcement layer. Figure 1 contains an illustration of the composite material „reinforced concrete".
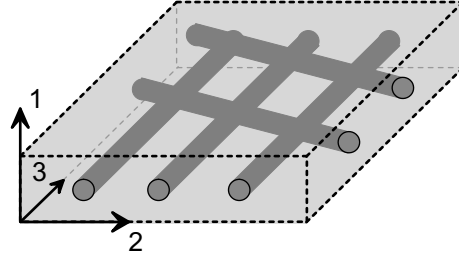
Figure 1: Illustration of the composite material.

Such a configuration is typical for reinforced shell-like as well as beam structures. Besides steel reinforcement also textile materials are frequently used as fiber-reinforcement in concrete structures. Such composite material may also be described within a micromechanical framework (Richter 2005). Therefore, the proposed micromechanical model presented in the following sections is formulated in a rather general format in order to consider a broad class of reinforcing materials.

3.2 *The representative volume element (RVE)*
A widely used approach in continuum micromechanics is based on the consideration of a representative volume element (RVE) representing an arbitrary material point of a structure. Thereby, the complex morphology of the microstructure is captured in a simplified manner by the RVE in order to estimate the related effective (macroscopic) response by means of an averaging procedure. To confirm the representative character of the RVE, the considered size l has to be large enough in order to ensure a statistical distribution of the constituents with a characteristic size d and at the same time it has to be essentially smaller than a length of the structure L

$$d \ll l \ll L. \qquad (10)$$

In Figure 2 the assumed RVE is depicted schematically. The considered microstructure is governed by two straight steel rebars with the tensor of elasticity $\boldsymbol{\mathcal{C}}_1, \boldsymbol{\mathcal{C}}_2$ and the related angles α_1, α_2, which are embedded in a continuous matrix (concrete) with the material tensor $\boldsymbol{\mathcal{C}}_m$. Depending on the position and volume fraction of each rebar, the expected effective mechanical response of the RVE is in general anisotropic or transversal isotropic. Hill's condition requires the equality of the energy on the micro and macro level independently of the constitutive law. This condition is a priori fulfilled by homogeneous strain boundary conditions applied by prescribing linear displacements at the boundary of the RVE (Zohdi and Wriggers 2005)

$$\boldsymbol{u}(\boldsymbol{x}) = \boldsymbol{\varepsilon}^* \cdot \boldsymbol{x}, \quad \boldsymbol{x} \in \partial V, \qquad (11)$$

where $\boldsymbol{\varepsilon}^*$ defines the macroscopic (constant) strain tensor.
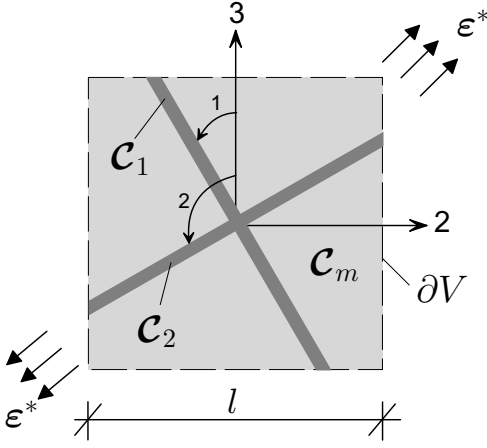
Figure 2: Representative volume element (RVE).

3.3 *Micro-macro mapping*

The local strain and stress fields within the RVE are averaged over the total volume V of the RVE in order to evaluate the homogenized values of the strains

$$< \boldsymbol{\varepsilon} >_V = \frac{1}{V} \int_V \boldsymbol{\varepsilon}(\boldsymbol{x}) \, \mathrm{d}V = \sum_{i=1}^n c_i < \boldsymbol{\varepsilon} >_i \qquad (12)$$

and of the stresses

$$< \boldsymbol{\sigma} >_V = \frac{1}{V} \int_V \boldsymbol{\sigma}(\boldsymbol{x}) \, \mathrm{d}V = \sum_{i=1}^n c_i < \boldsymbol{\sigma} >_i . \qquad (13)$$

Since the local averaged field values are assumed to be constant within each phase ($\boldsymbol{\sigma}_i = < \boldsymbol{\sigma}(\boldsymbol{x}) >_i$ and $\boldsymbol{\varepsilon}_i = < \boldsymbol{\varepsilon}(\boldsymbol{x}) >_i$), they can be summed up according to the volume fraction $c_i = V_i / V$, whereby V_i is the total volume of the phase i within the RVE. Hence, the volume of the RVE of the considered three-phase composite is assumed to be filled completely by all phases i.e. $c_1 + c_2 + c_m = 1$. According to the *average strain theorem*, for any perfectly bonded heterogeneous body the averaged strains $< \boldsymbol{\varepsilon} >_V$ given by equation (12) can be identified as the macroscopic strain tensor $\boldsymbol{\varepsilon}^*$ applied on the RVE i.e. $< \boldsymbol{\varepsilon} >_V = \boldsymbol{\varepsilon}^*$, which is independent of the considered constitutive laws (Zohdi and Wriggers 2005). For a three-phase composite, a reformulation of equation (12) and (13) leads to

$$\boldsymbol{\varepsilon}^* = < \boldsymbol{\varepsilon} >_V = c_1 \boldsymbol{\varepsilon}_1 + c_2 \boldsymbol{\varepsilon}_2 + c_m \boldsymbol{\varepsilon}_m \qquad (14)$$

describing the homogeneous macroscopic strains applied onto the composite material and to

$$\boldsymbol{\sigma}^* = < \boldsymbol{\sigma} >_V = c_1 \boldsymbol{\sigma}_1 + c_2 \boldsymbol{\sigma}_2 + c_m \boldsymbol{\sigma}_m \qquad (15)$$

for the macroscopic stresses representing the composite stress field. The related local stress tensor $\boldsymbol{\sigma}_i(\boldsymbol{\varepsilon}_i)$ is calculated according to each constitutive law given by equations (6) and (8). The unknown local strain fields $\boldsymbol{\varepsilon}_i$ have to estimated by means of the forth-order

localization (concentration) tensor $\boldsymbol{\mathcal{A}}_i$ which relates the homogenized macroscopic strains $\boldsymbol{\varepsilon}^*$ to the local strains within each phase

$$\boldsymbol{\varepsilon}_i = \boldsymbol{\mathcal{A}}_i : \boldsymbol{\varepsilon}^*, \quad i = 1, 2, m. \qquad (16)$$

The tensor $\boldsymbol{\mathcal{A}}_i$ of each phase accounts for the morphology of the microstructure by considering the elasticity, the volume fraction, the aspect ratio, the orientation and the shape of each constituent. It should emphasized that $\boldsymbol{\mathcal{A}}_i$ relates micro and macro quantities and depends therefore on the theory chosen for the micromechanical model. If a three-phase composite is considered only two concentration tensors have to be known. The third one can be determined from the average value

$$< \boldsymbol{\mathcal{A}} >_V = c_1 \boldsymbol{\mathcal{A}}_1 + c_2 \boldsymbol{\mathcal{A}}_2 + c_m \boldsymbol{\mathcal{A}}_m = \mathbb{1}, \qquad (17)$$

with $\mathbb{1}$ denoting the forth-order unit tensor. Due to different orientation and shape of the inhomogeneities, which is captured by $\boldsymbol{\mathcal{A}}_i$, the mechanical response of the related homogenized stiffness tensor $\boldsymbol{\mathcal{C}}^*$ is in general anisotropic even if all constituents are isotropic. As long as all constituents are in elastic regime, the mechanical constitutive relation for a composite material is defined by

$$\boldsymbol{\sigma}^* = \boldsymbol{\mathcal{C}}^* : \boldsymbol{\varepsilon}^*, \qquad (18)$$

where $\boldsymbol{\mathcal{C}}^*$ can be derived from the localization tensors of each phase

$$\boldsymbol{\mathcal{C}}^* = < \boldsymbol{\mathcal{C}} : \boldsymbol{\mathcal{A}} >_V = \sum_{i=1}^n c_i \boldsymbol{\mathcal{C}}_i : \boldsymbol{\mathcal{A}}_i. \qquad (19)$$

In the post-cracking range of the matrix or in the yielding regime of the rebars, however, the macroscopic tangent stiffness tensor of the composite $\boldsymbol{\mathcal{C}}^{*,tan}$ needs to be computed according to

$$\boldsymbol{\mathcal{C}}^{*,tan} = \mathrm{d}\boldsymbol{\sigma}^* / \mathrm{d}\boldsymbol{\varepsilon}^*. \qquad (20)$$

Depending on the considered micromechanical model the macroscopic tangent tensor $\boldsymbol{\mathcal{C}}^{*,tan}$ is obtained from linearization of each constitutive law

$$\boldsymbol{\mathcal{C}}_i^{tan} = \mathrm{d}\boldsymbol{\sigma}_i / \mathrm{d}\boldsymbol{\varepsilon}_i \quad i = 1, 2, m. \qquad (21)$$

3.4 *Three-phase* MORI-TANAKA *approach*

An appropriate homogenization scheme to derive the effective mechanical response of a RVE is provided by the widely used MORI-TANAKA approach (Mori and Tanaka 1973). This micromechanical model ensures continuity of the matrix phase and accounts for mechanical interactions between the inclusions in an average manner. According to this homogenization scheme, the reference material playing the predominant morphological role of the composite is the

continuous matrix. The inclusions and their states of strain and stress are directly affected by the matrix material. Within this approach, which is also denoted as *effective field theory*, the two limit cases (no inclusions exist ($c_i = 0$) and no matrix phase is considered ($c_m = 0$)) are covered by $\boldsymbol{\mathcal{C}}^* = \boldsymbol{\mathcal{C}}_m$ when $c_i = 0$ and $\boldsymbol{\mathcal{C}}^* = \boldsymbol{\mathcal{C}}_i$ when $c_m = 0$. In the following, the MORI-TANAKA equations for a non-linear three-phase composite are presented.

The relation between the strains of the phases $\boldsymbol{\varepsilon}_i$ and the applied macroscopic strains $\boldsymbol{\varepsilon}^*$ on the boundary of the RVE is formulated in the general format

$$\boldsymbol{\varepsilon}_i = \boldsymbol{\mathcal{A}}_i^{MT} : \boldsymbol{\varepsilon}^*, \quad i = 1, 2, m. \tag{22}$$

In order to identify the fourth-order concentration tensor $\boldsymbol{\mathcal{A}}_i^{MT}$ of each phase, the related assumptions of the MORI-TANAKA approach have to be taken into account. As mentioned before, the average strains of the inclusions ($\boldsymbol{\varepsilon}_1, \boldsymbol{\varepsilon}_2$) are defined by the average strains of the matrix $\boldsymbol{\varepsilon}_m$

$$\boldsymbol{\varepsilon}_1 = \boldsymbol{\mathcal{T}}_1 : \boldsymbol{\varepsilon}_m \quad \text{and} \quad \boldsymbol{\varepsilon}_2 = \boldsymbol{\mathcal{T}}_2 : \boldsymbol{\varepsilon}_m. \tag{23}$$

Based on ESHELBY's equivalent inclusion approach, the fourth-order tensor $\boldsymbol{\mathcal{T}}_i$ of each phase can be estimated by re-formulating the inclusion inhomogeneity problem as a homogeneous problem with eigenstrains (Eshelby 1957). The solution for a single elastic inhomogeneity with an ellipsoidal shape perfectly bonded to a surrounding homogeneous matrix is given by

$$\boldsymbol{\mathcal{T}}_i = \left[\boldsymbol{1\!1} + \boldsymbol{\mathcal{S}}^i : (\boldsymbol{\mathcal{C}}_m^{-1} : \boldsymbol{\mathcal{C}}_i - \boldsymbol{1\!1}) \right]^{-1} \quad i = 1, 2. \tag{24}$$

For an ellipsoidal geometry of the inclusions the forth-order ESHELBY tensor $\boldsymbol{\mathcal{S}}^i$ for each phase is solely dependent on the aspect ratio of the inclusion and on the Poisson's ratio ν_m of the surrounding isotropic matrix $\boldsymbol{\mathcal{C}}_m$. Since a cylindrical shape can be regarded as an ellipsoidal geometry with a special aspect ratio, the solution of the ESHELBY tensor in a local coordinate system $\boldsymbol{\mathcal{S}}^{loc}$ for the considered straight rebars can be computed (Eshelby 1957). In Figure 3, the cylindrical inhomogeneity representing a single rebar is illustrated. In this Figure, over-bars are used to characterize the local coordinate system. Note that the cross section of the rebar may have an elliptical or circular shape depending on the aspect ratio $s = a_2/a_1$. The ESHELBY tensor is transformed from the local to the global coordinate system within the 2-3-plane by means of the rotation tensor $\boldsymbol{Q}(\alpha)$

$$\mathcal{S}_{ijkl} = Q_{im}(\alpha) Q_{jn}(\alpha) Q_{ko}(\alpha) Q_{lp}(\alpha) \, \mathcal{S}_{mnop}^{loc}, \tag{25}$$

where α stand for the angle of rotation of the considered bar with respect to the positive x_1-axis (see Figure 2). For each set of rebars with the orientation α_i the related ESHELBY tensor $\boldsymbol{\mathcal{S}}^i$ has to be obtained
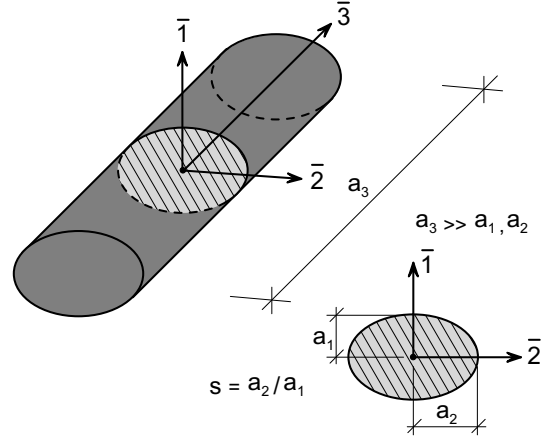
Figure 3: Representation of an inhomogeneity.

according to formula (25). The coordinate transformation of the stiffness tensors $\boldsymbol{\mathcal{C}}_m$ of the matrix and $\boldsymbol{\mathcal{C}}_i$ of the steel rebars is, because of the invariant property of isotropic tensors, not required.

As soon as the mechanical response of the matrix becomes inelastic, the related stiffness required for equation (24) is defined according to the actual damage state. In the post-cracking regime, the stiffness of the matrix phase degenerates to $\psi \boldsymbol{\mathcal{C}}_m$ where ψ is the remaining integrity, while the elastic stiffness of the steel reinforcement remains unchanged in the post-yielding regime. It should be noted that $\boldsymbol{\mathcal{T}}_i$ given by equation (24) also represents the localization tensor resulting from the dilute approach, where no interactions between inclusions are considered. The application of the dilute approach is limited to composites with very small volume fractions of the inclusions.

For the present three-phase composite the concentration tensors $\boldsymbol{\mathcal{A}}_i^{MT}$ introduced in equation (22) related to each phase can be identified from combining equation (19) for the homogenized effective material tensor $\boldsymbol{\mathcal{C}}^*$, equation (17) for the concentration tensors $\boldsymbol{\mathcal{A}}_i^{MT}$ together with equation (14) for the homogenized macroscopic strains $\boldsymbol{\varepsilon}^*$ and with the microscopic strains $\boldsymbol{\varepsilon}_i$ given by equation (23) as

$$\boldsymbol{\mathcal{A}}_1^{MT} = \left[c_1 \, \boldsymbol{1\!1} + c_2 \, \boldsymbol{\mathcal{T}}_2 : \boldsymbol{\mathcal{T}}_1^{-1} + c_m \, \boldsymbol{\mathcal{T}}_1^{-1} \right]^{-1} \tag{26}$$

$$\boldsymbol{\mathcal{A}}_2^{MT} = \left[c_1 \, \boldsymbol{\mathcal{T}}_1 : \boldsymbol{\mathcal{T}}_2^{-1} + c_2 \, \boldsymbol{1\!1} + c_m \, \boldsymbol{\mathcal{T}}_2^{-1} \right]^{-1} \tag{27}$$

$$\boldsymbol{\mathcal{A}}_m^{MT} = \left[c_1 \, \boldsymbol{\mathcal{T}}_1 + c_2 \, \boldsymbol{\mathcal{T}}_2 + c_m \, \boldsymbol{1\!1} \right]^{-1}. \tag{28}$$

Since $\boldsymbol{\mathcal{A}}_i^{MT}$ is a function of $\boldsymbol{\mathcal{T}}_1$ and $\boldsymbol{\mathcal{T}}_2$, it is obvious that the strains in each phase are affected by the other constituents, which allows for the consideration of micromechanical interactions within the MORI-TANAKA strategy.

3.5 Consideration of sets of reinforcement

The assumed RVE illustrated in Figure 2 considers two straight inhomogeneities (rebars) embedded in a

by modifying s
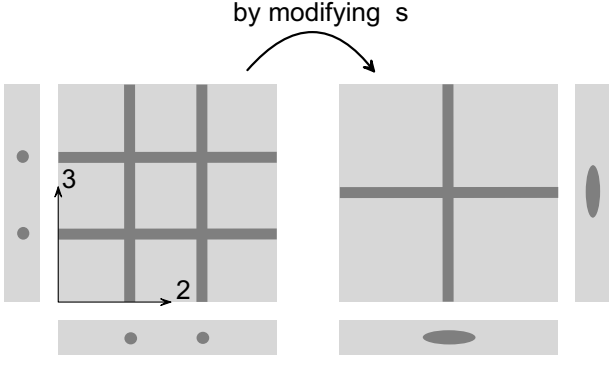
Figure 4: Consideration of reinforcement sets.

continuous matrix. If the distance between neighboring rebars is relatively large, the assumed mechanical response of the RVE containing single rebars in each direction is a suitable approximation of the macroscopic effective shear stiffness. Since the stiffness of the composite material in longitudinal direction of the rebars is manifested by a parallel system (VOIGT-boundary conditions), the adopted micromechanical model reproduces the proper stiffness in longitudinal direction independent of the distance between adjacent rebars. If sets of reinforcement are considered, however, depending on the distance between neighboring reinforcement bars, the effective shear stiffness may differ from the effective shear stiffness of a RVE whose size is in accordance with the requirements described in section 3.2.

The stiffening effect provided by the rebar in shear mode (dowel action) is frequently accounted for by increasing the effective shear stiffness of the composite according to beam bending mechanisms (Pietruszczak and Winnicki 2003; Linero et al. 2006). In the present approach, however, a consistent modification of the ESHELBY tensor $\mathcal{S}$ is performed in order to capture the effective shear stiffness when reinforcement sets embedded in a matrix are considered. To this end, the aspect ratio parameter $s = a_2/a_1$ specifying the cross section of the rebar is modified in order to reproduce the correct effective shear stiffness. It should emphasized, that this modification primarily affects the shear contribution while the macroscopic stiffness in longitudinal direction of the rebars remains unchanged. In Figure 4 the mapping from the standard RVE of a single set system to the modified RVE of sets of reinforcement bars is depicted schematically.

3.6 Homogenized mechanical response

For the proposed three-phase composite material, the macroscopic (homogenized) free energy Ψ^* can be additively decomposed into the matrix part Ψ_m and the part Ψ_i associated with the rebars according to

their volume fractions c_m and c_i, respectively

$$\Psi^* = c_m \Psi_m \mathbf{1} : \mathcal{A}_m^{MT-1} : \mathbf{1} + \sum_{i=1}^{2} c_i \Psi_i \mathbf{1} : \mathcal{A}_i^{MT-1} : \mathbf{1}. \quad (29)$$

Since the applied macroscopic strain tensor ε^* differs from the strains within each phase, the energetic consistency is ensured by taking the concentration tensor $\mathcal{A}_i^{MT}$ of the MORI-TANAKA scheme into account in equation (29). This approach can easily be confirmed by deriving the macroscopic stress tensor σ^* in equation (15) from the homogenized free energy Ψ^*

$$\begin{aligned}
\sigma^* &= \frac{\partial \Psi^*}{\partial \varepsilon^*} = c_m \frac{\partial \Psi_m}{\partial \varepsilon^*} : \mathcal{A}_m^{MT-1} + \sum_{i=1}^{2} c_i \frac{\partial \Psi_i}{\partial \varepsilon^*} : \mathcal{A}_i^{MT-1} \\
&= c_m \frac{\partial \Psi_m}{\partial \varepsilon_m} : \frac{\partial \varepsilon_m}{\partial \varepsilon^*} : \mathcal{A}_m^{MT-1} + \sum_{i=1}^{2} c_i \frac{\partial \Psi_i}{\partial \varepsilon_i} : \frac{\partial \varepsilon_i}{\partial \varepsilon^*} : \mathcal{A}_i^{MT-1} \\
&= c_m \sigma_m : \underbrace{\mathcal{A}_m^{MT} : \mathcal{A}_m^{MT-1}}_{\mathbb{1}} + \sum_{i=1}^{2} c_i \sigma_i : \underbrace{\mathcal{A}_i^{MT} : \mathcal{A}_i^{MT-1}}_{\mathbb{1}} \\
&= c_m \sigma_m + \sum_{i=1}^{2} c_i \sigma_i \overset{!}{=} < \sigma >_V .
\end{aligned} \quad (30)$$

The homogenized non-linear tangent operator $\mathcal{C}^{*,tan}$ relating macro-strains to the macro-stresses is identified as

$$\begin{aligned}
\mathcal{C}^{*,tan} &= \frac{d\sigma^*}{d\varepsilon^*} = c_1 \frac{d\sigma_1}{d\varepsilon^*} + c_2 \frac{d\sigma_2}{d\varepsilon^*} + c_m \frac{d\sigma_m}{d\varepsilon^*} \\
&= c_1 \frac{d\sigma_1}{d\varepsilon_1} : \frac{d\varepsilon_1}{d\varepsilon^*} + c_2 \frac{d\sigma_2}{d\varepsilon_2} : \frac{d\varepsilon_2}{d\varepsilon^*} + c_m \frac{d\sigma_m}{d\varepsilon_m} : \frac{d\varepsilon_m}{d\varepsilon^*} \\
&= c_1 \mathcal{C}_1^{tan} : \mathcal{A}_1^{MT} + c_2 \mathcal{C}_2^{tan} : \mathcal{A}_2^{MT} + c_m \mathcal{C}_m^{tan} : \mathcal{A}_m^{MT} \\
&= \mathcal{C}_m^{tan} + c_1(\mathcal{C}_1^{tan} - \mathcal{C}_m^{tan}) : \mathcal{A}_1^{MT} + \\
&\quad c_2(\mathcal{C}_2^{tan} - \mathcal{C}_m^{tan}) : \mathcal{A}_2^{MT}.
\end{aligned} \quad (31)$$

The tangent stiffness of each phase $\mathcal{C}_i^{tan}$ depends on the damage or yielding state and is calculated according to the adopted material model for each phase. Note, that in the non-linear regime, also the concentration tensor $\mathcal{A}_i^{MT}$ is affected by the damage or yielding state, which is manifested by $\mathcal{T}_i$ given in equation (24). As long as all constituents are within the elastic range however, equation (31) coincides with equation (19) and the classical micromechanical laws of elastic composites are valid.

3.7 Numerical study in the elastic regime

To illustrate the influence of the volume fraction and the orientation of the rebar on the effective stiffness $\mathcal{C}^*$ within the elastic regime of both constituents, a simple benchmark test is performed. To this end, one single rebar with Young's modulus $E_s = 76,000 \text{ N/mm}^2$ and Poissons ratio $\nu_s = 0.2$ is embedded within a matrix with $E_m = 30,000 \text{ N/mm}^2$ and
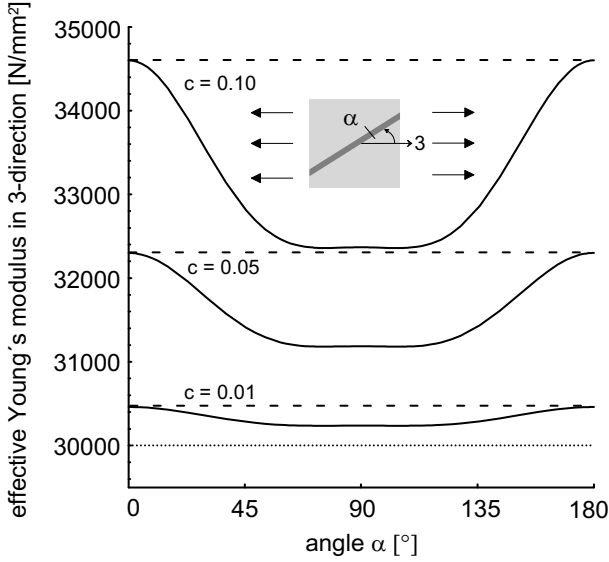
Figure 5: E_3^* for different volume fractions c (numerical).

$\nu_m = 0.2$. The shape of the rebar is assumed to be cylindrical (aspect ratio $s = 1$). For different angles α of the rebars, the effective Young's modulus in 3-direction $E_3^* = 1/\mathcal{C}_{33}^{*-1}$ is computed for three different volume fractions of the rebar ($c = 1/5/10\%$).

Two homogenization procedures - the *mixture theory* and the MORI-TANAKA approach - are used. Since in the *mixture theory* besides the volume fraction no micromechanical information is considered, the related equations are directly obtained by assuming $\mathcal{A} = \mathbb{1}$ for the concentration tensor leading to an isotropic homogenized stiffness tensor $\mathcal{C}^*$. The mechanical response obtained with the MORI-TANAKA technique, however, is manifested by an anisotropic stiffness even if all constituents are isotropic. Figure 5 illustrates the isotropic response based on the *mixture theory* (dashed lines) and the more realistic anisotropic, orientation-dependent response obtained from the MORI-TANAKA approach (solid lines). Since the *mixture theory* is based on a parallel system of the constituents, resulting in uniform (constant) strains within the RVE, the approximated macroscopic stiffness constitutes an upper bound (VOIGT approximation). In addition to the orientation also the volume fraction of the rebar c strongly affects the homogenized effective stiffness.

3.8 *Homogenization within multi-physics*

In this section, the extension of the adopted (mechanical) homogenization technique for reinforced concrete to a multi-phase model for concrete is briefly addressed. Since the free energy of the porous matrix Ψ_m given in equation (1) is governed by the moisture content m_l and by the absolute temperature T, the related state equations of the liquid pressure p_l and of the entropy S

$$p_l = \rho_l\, \partial\Psi^*/\partial m_l = \rho_l\, c_m \partial\Psi_m/\partial m_l\, \mathbf{1}:\mathcal{A}_m^{MT-1}:\mathbf{1} \quad (32)$$

Table 1: Mechanical material parameters.

Concrete			Steel		
E_m	=	20,000 MPa	E_s	=	200,000 MPa
ν_m	=	0.2	ν_s	=	0.3
f_m^c	=	20 MPa	σ_y	=	442 MPa
f_m^t	=	1.0 MPa	K	=	0 MPa
G_f	=	0.1 N/mm	s	=	100

$$S = -\partial\Psi^*/\partial T = -c_m \partial\Psi_m/\partial T\, \mathbf{1}:\mathcal{A}_m^{MT-1}:\mathbf{1} \quad (33)$$

can derived from the free energy of the composite material Ψ^* given in equation (29). It is implicitly assumed that moisture and heat transport are not affected by the embedded reinforcement. The expressions for $\partial\Psi_m/\partial m_l$ and $\partial\Psi_m/\partial T$ can be found in (Grasberger and Meschke 2004).

4 EXPERIMENTAL VERIFICATION

A re-analysis of a shear test of a bi-directionally reinforced panel tested experimentally (Collins et al. 1985) is performed in order to validate the proposed model for reinforced concrete. The considered panel PV27 with dimensions $890 \cdot 890 \cdot 70\ mm^3$ is reinforced homogeneously with a volume fraction of 1.785% in each orthogonal direction. For this panel, the finite element discretization contains elements with identical material parameters for the composite. While the experiment has been performed load-controlled the finite element analysis is performed displacement-controlled. A relatively large amount of reinforcement and a low concrete strength have been chosen to provoke structural concrete shear failure (Collins et al. 1985). The material parameters for the concrete matrix material and for the reinforcing steel are collected in Table 1, with f_m^c and f_m^t representing the compression and tensile strength, respectively and G_f is the fracture energy. For the steel an ideal elasto-plastic behaviour is assumed. At the boundaries of the investigated panel, the concrete and the reinforcing rebars are perfectly bonded. The stiffening effect of the reinforcing steel sets is captured according to section 3.5 by modifying the aspect ratio of the cross section s.

The structural shear-stress versus the equivalent shear-strain behaviour is depicted in Figure 6. The structural shear-strains are computed from the prescribed displacements at the top of the panel, and the structural shear-stresses are obtained by averaging the shear-stresses calculated also at the top at the panel. The comparison between the experimental and numerical result shows a satisfactory agreement. The onset of cracking within the matrix is well predicted by the proposed model. The maximum shear-stress, however, is slightly underestimated in the numerical analysis by $\sim 10.8\%$. As reported in (Collins et al. 1985) and also confirmed by the numerical analysis, structural failure of the panel originates from concrete
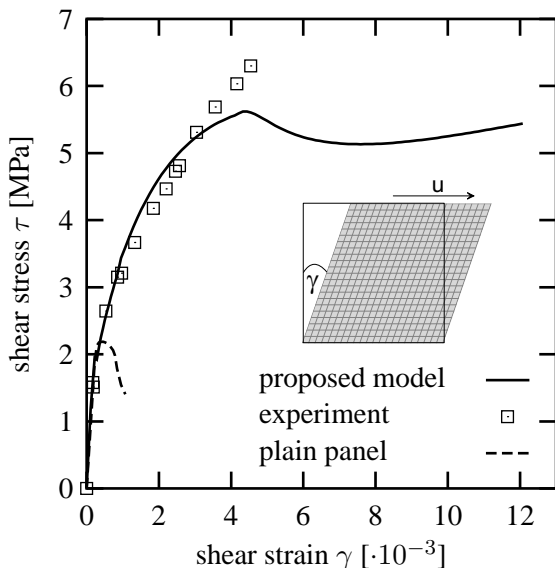
Figure 6: Analysis of an orthogonally reinforced shear panel (Collins et al. 1985).

crushing. No yielding of reinforcement is observed. In order to illustrate the contribution of the rebars to the global shear stiffness, the same concrete panel without consideration of reinforcement is also analyzed numerically. The respective shear stress-shear strain curve is included in Figure 6. Since the stiffening effect provided by the reinforcement is missing, the maximum load capacity is controlled by matrix cracking. The maximum capacity of the plain concrete panel is approximately one third of the reinforced panel (Figure 6).

5 CONCLUDING REMARKS

In this paper, a constitutive model for reinforced concrete based on continuum micromechanics is presented. Reinforced concrete is represented as a three-phase composite material, characterized by a continuous concrete matrix and two different sets of steel reinforcement rebars. The MORI-TANAKA homogenization scheme is considered as a suitable approach to derive the homogenized constitutive relations of the composite material and to obtain related local (micromechanical) field information. Dowel action between the reinforcement bars and the concrete is implicitly captured by the chosen approach. The proposed model is formulated within a poromechanics framework developed for durability-oriented numerical analysis of reinforced concrete structures. However, in the present paper the main focus has been laid on the purely mechanical response of reinforced concrete. Since the work is still in progress, debonding mechanisms between concrete and the embedded reinforcement (bond slip) as well as corrosion have not yet been taken into account.

REFERENCES

Bažant, Z. P., A. B. Hauggaard, S. Baweja, and F.-J. Ulm (1997). Microprestress-solidification theory for concrete creep. I: Aging and drying effects. *Journal of Engineering Mechanics (ASCE) 123*(11), 1188–1194.

Collins, M. P., F. J. Vecchio, and G. Mehlhorn (1985). An international competition to predict the response of reinforced concrete panels. *Canadian Journal of Civil Engineering 12*, 624–644.

Coussy, O. (2004). *Poromechanics*. Chichester, England: Wiley.

Eshelby, J. D. (1957). The determination of the elastic field of an ellipsoidal inclusion, and related problems. *Proc. Roy. Soc. London, Series A, 241*, 376–396.

Grasberger, S. and G. Meschke (2003). Drying shrinkage, creep and cracking of concrete: From coupled material modelling to multifield structural analyses. In R. De-Borst, H. Mang, N. Bićanić, and G. Meschke (Eds.), *Computational Modelling of Concrete Structures*, pp. 433–442. Balkema.

Grasberger, S. and G. Meschke (2004). Thermo-hygro-mechanical degradation of concrete: From coupled 3D material modelling to durability-oriented multifield structural analyses. *Materials and Structures 37*, 244–256.

Linero, D. L., J. Oliver, A. E. Huespe, and M. D. G. Pulido (2006). Cracking modeling in reinforced concrete via the strong discontinuity appoach. In G. Meschke, R. de Borst, H. A. Mang, and N. Bićanić (Eds.), *Computational Modelling of Concrete Structures*, London, pp. 173–182. Taylor & Francis Group.

Meschke, G. and S. Grasberger (2003). Numerical modeling of coupled hygromechanical degradation of cementitious materials. *Journal of Engineering Mechanics (ASCE) 129*(4), 383–392.

Meschke, G., R. Lackner, and H. A. Mang (1998). An anisotropic elastoplastic-damage model for plain concrete. *International Journal for Numerical Methods in Engineering 42*, 703–727.

Mori, T. and K. Tanaka (1973). Average stress in the matrix and average elastic energy of materials with misfitting inclusions. *Acta Metall. 21*(5), 571–574.

Pietruszczak, S. and A. Winnicki (2003). Constitutive Model for Concrete with Embedded Sets of Reinforcement. *Journal of Engineering Mechanics 129*(7), 725–738.

Richter, M. (2005). *Entwicklung mechanischer Modelle zur analytischen Beschreibung der Materialeigenschaften von textilbewährtem Feinbeton*. Ph. D. thesis, TU Dresden, Germany.

Simo, J. C. and T. J. R. Hughes (1998). *Computational inelasticity*. Berlin: Springer.

Zaoui, A. (2002). Continuum Micromechanics: Survey. *Journal of Engineering Mechanics 128*(8), 808–816.

Zohdi, T. I. and P. Wriggers (2005). *Introduction to Computational Micromechanics*. Springer.